Description of new micro-colonial fungi species *Neophaeococcomyces mojavensis*, *Coniosporium tulheliwenetii, and Taxawa tesnikishii* cultured from biological soil crusts

Tania Kurbessoian[1], Sarah A. Ahmed[2], Yu Quan[2], Sybren de Hoog[2], Jason E. Stajich [1,*]
[1]*Department of Microbiology and Plant Pathology and Institute of Integrative Genome Biology, University of California, 92521, Riverside, CA, USA*
[2]*Radboudumc/CWZ Ceter of Expertise for Mycology, Nijmegen, 6525GA Nijmegen, The Netherlands*

*Correspondence: jason.stajich@ucr.edu; Tel.: +1 951.827.2363 (J.E.S.)

Abstract

Black yeasts and relatives comprise Micro-Colonial Fungi (MCFs) which are slow-growing stress-tolerant micro-eukaryotes that specialize in extreme environments. MCFs are paraphyletic and found in the Orders *Chaetothyriales* (*Eurotiomycetes*) and *Dothideales* (*Dothidiomycetes*). We have isolated and described three new MCFs species from desert biological soil crusts (BSCs) collected from two arid land regions: Joshua Tree National Park (Mojave Desert) and UC Natural Reserve at Boyd Deep Canyon (confluence of Mojave and Sonoran Deserts). BSCs are composite assemblages of cyanobacteria, eukaryotic algae, fungi, lichens, and bryophytes embedded into the surface of desert soils, providing a protective buffer against the harsh desert environment. Our work focused on one type of desert BSC, the cyanolichen crust dominated by *Collema sp.* Using culture-dependent protocols, three MCFs were axenically isolated from their respective samples along with the extracted DNA. Their genomes were sequenced using Illumina and Nanopore, and finally assembled and annotated using hybrid assembly approaches and established bioinformatics pipelines to conduct final taxonomic phylogenetic analysis and placement. The three species described here are unique specimen from desert BSCs, here we introduce, *Neophaeococcomyces*

mojavensis (*Chaetothyriales)*, *Cladosporium tulheliwenetii* (*Dothideales*), and *Taxawa tesnikishii* (*Dothideales*).

Introduction

Biological Soil Crusts

Dryland ecosystems constitute some of the largest terrestrial biomes, collectively covering 47.2% of Earth's land surface (6.15 billion hectares) (Lal 2004). Drylands are expanding due to climate change and population pressures, while also supporting over 38% of the global human population (Lal 2004; Maestre et al. 2012). Biological Soil Crusts (BSCs) cover up to 70% of dryland ecosystems (Rozenstein and Karnieli 2015). They are an ancient feature of dryland ecosystems, with the earliest known fossil records indicating nearly 2.6 billion years ago (Beraldi-Campesi and Retallack 2016). The initial phases of BSC formation in drylands are the stabilization of the soil surface by filamentous cyanobacteria, followed by the colonization of lichens and bryophytes (Weber et al. 2016). Within dryland ecosystems, the carbon and nitrogen dynamics are often described as the "pulse-reserve model" where precipitation events happen sporadically, stimulating intermittent biological activity which generates biomass and organic matter. After extended periods of heat and dryness, the biological activity goes into reserve and becomes dormant again (Pietrasiak et al. 2013). BSCs also increase soil fertility by increasing soil stability and adding fixed atmospheric carbon and nitrogen to the soil underneath, allowing for greater complex microbial and micro-faunal populations (Housman et al. 2007).

Within BSCs is a consortium of cyanobacteria, algae, diazotrophic bacteria, lichen, fungi, and bryophytes that colonize and stabilize the soil surfaces against natural forces like wind and water

(Warren et al. 2019). These microorganisms recruit partners to create a mutualistic symbiotic relationship which helps maintain a self-sustaining micro-ecosystem. Phototrophic organisms fix carbon that is later used by surrounding micro-organisms as an energy source (Green et al. 2016). The presence of chemoheterotrophic bacteria and cyanobacteria indicates that BSCs are capable of fixing atmospheric nitrogen to increase levels of fixed nitrogen for nearby living vascular plants (Belnap and Harper 1995; Evans and Ehleringer 1993). BSCs have been shown to reduce surface erodibility as filaments of cyanobacterial sheath material lipopolysaccharides (LPS) entangle surface particles and create a crust that is more resistant to entrainment than the layers below (Lal 2004).

Different ecological sites promote different crust taxa. BSCs are classified into types based on the dominant photosynthetic microorganism in the crust which includes: cyanobacteria, algae, lichens, or mosses to produce Cyano-Lichenized Crust, Light Algal Crusts, Dark Algal Crusts, Lichenized Crust, Rough Moss Crust and Smooth Moss Crust (Pietrasiak 2005). The community types are classified based on dominant taxa and their distinct morphologies (Pietrasiak et al. 2013). BSC's main roles include: 1) mediating almost all inputs and outputs (gasses, nutrients, water) to and from the strata above and below the surface, 2) being the zone of high nutrient deposition, transformation, and availability, 3) structuring temporal, spatial, and compositional aspects of the surrounding vascular plant community, and 4) facilitating the direct delivery of carbon, nutrients, and water by BSCs from the soil interspace to nearby vascular plants.

73 *Micro-colonial Fungi*

74 'Black yeasts and relatives' comprise a large amalgamate of melanized fungi. Among these are
75 micro-colonial fungi (MCF) or rock-inhabiting fungi (RIF), prevalent names used to describe a
76 special group of melanized fungi. Micro-colonial fungi are ubiquitous and found in the most
77 extreme environments. They are present in widely divergent habitats, such as on the indoor rubbers
78 of dishwashers, in oil deposits, on the surfaces of Mediterranean monuments, on the radioactive
79 walls of the Chernobyl Station, in mutilating skin infections in third-world countries, in human
80 superficial and invasive infections, or colonizing lungs of cystic fibrosis patients (de Hoog et al.
81 2005; Hoog et al. 2000; Vicente et al. 2008; Gümral et al. 2014; Saunte et al. 2012; Thanh and
82 Hien 2019; Mehdiabadi and Schultz ; Little and Currie 2008; de Hoog and Hermanides-Nijhof
83 1977). MCFs are compelling not only because of where we can discover them and their unique
84 physiological features, but also because of how little we know about them.

85

86 MCFs have three main characteristics: meristematic growth, presence of 1,8-DHN melanin, and
87 membrane-associated carotenoids and intracellular mycosporine-like amino acids (Staley et al.
88 1982; Gorbushina et al. 2003). These features distinguish them from other fungi, yet
89 phylogenetically they fall into two paraphyletic Ascomycota clades, the *Dothideomycetes* and
90 *Chaetothyriomycetes*. Melanin is a highly complex secondary metabolite that is produced by many
91 organisms through different evolutionary lineages (Siletti et al. 2017; Wheeler 1983). Most
92 importantly in MCFs, it has been used as a virulence factor as a non-specific armor against host
93 immune system to infect its host (Steenbergen and Casadevall 2003; Casadevall et al. 2003;
94 Casadevall et al. 2000; Nosanchuk et al. 2015; Taborda et al. 2008; Gómez and Nosanchuk 2003).

95 Available research indicates melanin has other functional roles, such as metal chelation,
96 photoprotection, protection from heat and cold stress, binding to antifungals to reduce efficacy,
97 radioprotection (physical shielding and quenching of cytotoxic free radicals), protection from
98 desiccation, interacting with a range of electromagnetic radiation frequencies and mechanical-
99 chemical cellular strength (Dadachova et al. 2008; Casadevall et al. 2003; Gorbushina et al. 2003).
100 Understanding poorly studied fungal function in one extreme environment could yield insight into
101 MCF adaptation in other extreme environments.
102
103 The objective of this study was to collect MCF from biological soil crust samples from desert
104 drylands. During our collection, we isolated 3 MCF that had not been described previously. Our
105 efforts to converse with indigenous tribes allowed us to provide a new naming scheme for our
106 strains. We also used a new methodology described herein using BUSCO nucleotide and amino
107 acid sequences to build a multi-locus phylogenetic tree, which proved to be similar to a more
108 conventional tree of MCF which used four highly conserved markers.
109
110 **Materials and Methods**
111 *Sampling*
112 Biological soil crusts were collected from two locations in Southern California. The first crust
113 location at the northern edge of Joshua Tree National Park. The second crust location was from
114 Boyd Deep Canyon, near the campgrounds in the UC Natural Reserve. Metadata and coordinates
115 can be found in **Table 1**. All materials were collected under permits from the BLM or permission
116 of the UC National Reserves.
117

118 *Culturing and isolation*

119 Media for isolation, cultivation, and collection used were Malt Extract Yeast Extract (MEYE)
120 media for nutrient-rich complex media and nutrient-poor, oligotrophic media Glucose Asparagine
121 Agar (GAA). The recipe for both media can be found in our protocols.io and the step-by-step
122 protocol for culturing MCFs (Kurbessoian 2019)). The mixing of the sample with the media
123 provides an environment with different layers of dissolved oxygen. Fast-growing fungi require full
124 oxygenation and grow on the surface of the media, while slow-growing MCFs propagate on the
125 bottom of the culture plate, requiring low levels of oxygen. This also allowed a much easier way
126 to culture and select the strains. Once grown, axenic MCFs were isolated by using a flamed loop
127 to pick and place onto clean media.

128
129 *Morphological analysis*

130 Strains were grown on Malt Extract Agar (MEA; Oxoid, England), Oatmeal Agar (OA; Oxoid)
131 and Potato dextrose Agar (PDA; Sigma, Germany) incubated at 28°C for 14 days under UV light.
132 Colonies were photographed with a Nikon C-DSD230 dissecting microscope. Microscopic mounts
133 were made in lactic acid and examined using a light microscope (Nikon Eclipse 80i). Pictures were
134 taken with a digital camera (Nikon Digital Sight, DS-5M) and adjusted in Adobe Photoshop CS.

135
136 *DNA extraction*

137 Each isolate was grown on MEYE for approximately 1.5 weeks at 22°C. Genomic DNA was
138 extracted from hyphae collected from MEYE plates using the CTAB protocol described in our
139 protocols.io document (Carter-House et al. 2020). Melanin was removed using multiple iterations
140 of phenol:chloroform and chloroform washes of our sample. Genomic DNA was measured by

141 Nanodrop and diluted to ~28ng/µl. DNA extractions were sent to the UCR Genomics core
142 (Riverside, CA) for 2x150bp sequencing on an Illumina NovoSeq 6000. DNA from all three
143 isolates was also extracted and sequenced on Oxford Nanopore (ONT) platform with library
144 preparation and sequencing following the manufacturer's directions (Oxford Nanopore, Oxford
145 United Kingdom). Flow cell versions FAK68780, FAQ05493, FAL40904, and FAL35715 were
146 used along with base-calling on the cluster using guppy (*v.3.4.4.+a296cb*) (Wick et al. 2019).
147
148 *ITS sequencing*
149 To identify the isolates, extracted DNA was used as a template for PCR amplification using fungal
150 primers ITS1-F (CTTGGTCATTTAGAGGAAGTAA) and ITS4
151 (TCCTCCGCTTATTGATATGC) along with the PCR setup. PCR was performed in 25 µL
152 reaction volumes using 12.5 µL of Taq 2X MasterMix (NEB), 9.5µL water, 1µL of 20 picomol
153 ITS1-F, 1µL of 20 picomol ITS4 and 1µL of template DNA. Using Bio-Rad thermal cycler, the
154 samples were passed through denaturation and enzyme activation at 95°C for 5 minutes, followed
155 by amplification for 35 cycles at the following conditions: 30 seconds at 95°C, 1 minute at 72°C,
156 and 30 seconds at 65°C. A final 5-minute extension at 72°C completes the protocol. PCR results
157 typically yield between 50-60 ng of amplified DNA.
158 *Genome assembly and annotation*
159 Initial genome assemblies were constructed for the three MCF isolates using Illumina sequencing.
160 Each MCF was also re-sequenced using Oxford Nanopore technology. All genomes were *de novo*
161 assembled with the AAFTF pipeline (*v.0.2.3*) (Palmer and Stajich 2022) which performs read QC
162 and filtering with BBTools bbduk (*v.38.86)* (Bushnell 2014) followed by SPAdes (*v.3.15.2*)

163 (Bankevich et al. 2012) assembly using default parameters, followed by screening to remove short
164 contigs < 200 bp and contamination using NCBI's VecScreen. The BUSCO ascomycota_odb10
165 database (Manni et al. 2021) was used to determine how complete the assembly 3 isolates were. A
166 hybrid assembly of each was generated using MaSUrCa *(v.3.3.4)* (Zimin et al. 2013) as the
167 assembler using both Nanopore and Illumina sequencing reads. General default parameters were
168 used except: CA_PARAMETERS=cgwErrorRate=0.15, NUM_THREADS=16, and
169 JF_SIZE=200000000.
170
171 We predicted genes in each near-complete genome assembly with Funannotate (*v1.8.1*) (Palmer
172 and Stajich 2020). A masked genome was created by generating a library of sequence repeats with
173 the RepeatModeler pipeline (Smit and Hubley 2008). These species-specific predicted repeats
174 were combined with fungal repeats in the RepBase (Bao et al. 2015) to identify and mask repetitive
175 regions in the genome assembly with RepeatMasker (*v.4-1-1*) (SMIT 2004). To predict genes, *ab*
176 *initio* gene predictors SNAP (*v.2013_11_29*) (Korf 2004) and AUGUSTUS (*v.3.3.3*) (Stanke et al.
177 2006)were used along with additional gene models by GeneMark.HMM-ES (*v.4.62_lic*) (Brůna et
178 al. 2020), and GlimmerHMM (*v.3.0.4*) (Majoros et al. 2004) utilize a self-training procedure to
179 optimize *ab initio* predictions. Additional exon evidence to provide hints to gene predictors was
180 generated by DIAMOND BLASTX alignment of SwissprotDB proteins and polished by Exonerate
181 (*v.2.4.0*) (Slater and Birney 2005). Finally, EvidenceModeler (*v.1.1.1*) (Haas et al. 2008) generated
182 consensus gene models in Funannotate that were constructed using default evidence weights. Non-
183 protein-coding tRNA genes were predicted by tRNAscan-SE (*v.2.0.9*) (Lowe and Chan 2016).
184

185 The annotated genomes were processed with antiSMASH (*v.5.1.1*) (Blin et al. 2021) to predict
186 secondary metabolite biosynthesis gene clusters. These annotations were also incorporated into
187 the functional annotation using Funannotate. Putative protein functions were assigned to genes
188 based on sequence similarity to InterProScan5 (*v.5.51-85.0*) (Jones et al. 2014), Pfam (*v.35.0*)
189 (Finn et al. 2014), Eggnog (*v.2.1.6-d35afda*) (Huerta-Cepas et al. 2019), dbCAN2 (*v.9.0*) (Zhang
190 et al. 2018) and MEROPS (*v.12.0*) (Rawlings et al. 2018) databases relying on NCBI BLAST
191 (*v.2.9.0+)* (Sofi et al. 2022) and HMMer (*v.3.3.2*) (Potter et al. 2018). Gene Ontology terms were
192 assigned to protein products based on the inferred homology based on these sequence similarity
193 analyses. The final annotation produced by Funannotate was deposited in NCBI as a genome
194 assembly with gene model annotation.
195
196 Sequence Read Archive (SRA) files and genome assembly and annotation files can be found under
197 BioProject PRJNA631111.
198
199 *Mating type determination*
200 The Mating Type (MAT) locus was identified by searching for homologous MAT genes. The
201 identified homologous regions were examined for their conserved synteny of the MAT locus using
202 clinker (Gilchrist and Chooi 2021) and a custom Biopython script (Cock *et al.* 2009) (Kurbessoian
203 2022) to extract the annotated region of the genome which contained the locus.
204
205 *Telomeric repeat determination*
206 Identification of telomeric repeat sequences was performed using the FindTelomeres.py script
207 (https://github.com/JanaSperschneider/FindTelomeres). Briefly, this searches for chromosomal

208 assembly with a regular expression pattern for telomeric sequences at each scaffold's 5' and 3'
209 end. Telomere repeat sequences were also predicted using the Telomere Identification toolkit (tidk)
210 (*v.0.1.5*) "explore" option (https://github.com/tolkit/telomeric-identifier).
211
212 *Inferring phylogenetic relationships of species*
213 Inference of the species relationship was made through phylogenetic trees containing the three
214 new MCF strains described here and available named species with sequence data.
215
216 A multi-gene tree was generated using collected BT2 (Beta-Tubulin), CAM (Calmodulin), ITS
217 (Inter-Transcribed Spacer), and LSU (Large Subunit) genes from a total of 32 species. These
218 samples were chosen to compare to the three MCF species with closely related species to confirm
219 identification as a novel lineage. The final selection of 32 species was based on iterations of
220 sequence searching and tree building data analyses to determine close relatives. To include genes
221 from genomes, genome assemblies were searched by TBLASTN tool of NCBI-BLAST (*v.2.9.0+*)
222 using *Zymoseptoria tritici* genes (AAS55060.1 for Beta tubulin) and (AEI69650.1 for
223 Calmodulin). The collection of ITS and LSU genes were obtained from NCBI-Genbank based on
224 BLASTN searches. Each gene file contained FASTA formatted sequences from each species or
225 isolate, the sequences were aligned with MUSCLE (*v.5.1*) and trimmed for low quality alignment
226 regions using Clipkit (*v.1.3.0).* Nucleotide substitution models were determined for each alignment
227 with IQTREE2. The alignments were combined into a single 'supermatrix' alignment with
228 combine_multiseq_aln.py script provided in PHYling. The script also produced a partition file
229 listing the sub-locations of each marker gene alignment in the super-alignment. IQTree2 was run
230 to find a substitution model fit for and partition merging. To reduce the computational burden that

occurs with including a large number of organism ribosomal sequences we used the relaxed hierarchical clustering algorithm (Lanfear et al. 2014) using the tag -m MF+MERGE and running 1000 bootstrapping on the alignment.

Choosing to work with indigenous tribes

Our choice for naming of the three MCFs isolated from BSCs is rooted in the traditional indigenous land where these were found. *Neophaeococcomyces mojaviensis* was isolated from BSCs collected from the south-east region of Joshua Tree National Park, territories ancestral to Yuhaaviatam/Maarenga'yam (Serrano) and Newe Segobia (Western Shoshone) Tribes (Brown and Boyd 1922; Kroeber 1925). The isolates of *Coniosporium tulheliwenetii* and *Taxawa tesnikishii* were isolated from BSCs collected from UC Reserve Boyd Deep Canyon (Reserve doi:10.21973/N3V66D), land of the traditional ancestral Cahuilla Tribe (White 2001; Hooper 1920). The word *tulheliweneti* in Cahuilla means, black-spread-be-noun, while *Taxaw* means body, and *tesnikish* means yellow. In Cahuilla traditions, Taxaw tesnikish is the deity that resided in Boyd Deep valley. To recognize the origins, we consulted with Tribal linguists and speakers to derive their names from Cahuilla and Serrano terms that describe either geographic region, oral tradition, or features that help distinguish them.

Results

Biological soil crust collection

Biological soil crusts were collected from the two regions described in **Table 1**. The method of sterile collection is through the use of sterile empty Petri dishes, stamped on top, with a sterile

253 spatula used to grab the soil from underneath, flip the sample into the dish, place the lid on top and
254 seal it with parafilm.

255 *Culturing results*

256 Samples material was used to culture fungi using a collection of techniques in our laboratory at
257 UC Riverside. More than 50+ fungal culture specimens were collected from biological soil crusts,
258 18 were MCF cultures. The pour plate protocol used allows for fast-growing fungi to appear on
259 the top, while MCF grows within the bottom layer of media in Petri dishes. Samples were excised
260 from deep in the media and allowed to grow on fresh MEYE. Each sample had the DNA extracted
261 and each strain ITS was Sanger sequenced to determine the identity. JES_112 was initially
262 identified as a *Knufia* species. JES_115 and JES_119 were identified as *Dothideales* species, but
263 there remained ambiguity on the exact species identification as a near perfect sequence match was
264 not found for ITS1 to assign a name.

265 *Sequencing and assembly of MCF isolates*

266 To gain information on the genome content for the recovered MCF isolates, we sequenced and
267 assembled the genomes of the three isolates (**Table 2**). Each isolate was sequenced with Illumina
268 MiSeq and Oxford Nanopore (ONT) technology and constructed into a hybrid assembly that
269 combined both read types (**Table 2)**. The depth of coverage ranged from 25-43x Illumina coverage
270 across the three specimens, while Nanopore ranged from 0.83-194.58x. Assessment of the genome
271 completeness was performed with BUSCO (Benchmarking Universal Single-Copy Orthologs) and
272 results indicated the genomes had ranges of 73-92.9% complete gene copies found, with 73-92.8%
273 of the markers appearing as single copies in the assembly, a low fraction of duplication (0.1-0.2).
274 Contig counts ranged from 38-480, while the average genome assembly size is about 30 Mbps for

275 all isolates. The L50 statistic, a measure of the count of the smallest number of contigs whose sum
276 makes up half of the genome size, ranged from 9-88, and the N50 statistic, a measure of the
277 smallest contig length for covering half of the genome size, ranging from 117kbp - 1.232 Mbp.
278 To further assess completeness, we tested for the presence of telomeric repeat units
279 "TTTAGGG/CCCTAA". These were identified as repeat arrays at both ends of contigs in JES_115
280 and JES_119, 61 total telomeres and 55 total telomeres respectively, though the results were
281 inconclusive for JES_112. No telomeric repeat-containing contigs were detected in JES_112
282 which could be due to the fragmented nature of the genome assembly. The fragmented assembly
283 also is reflected in the lower BUSCO score for this genome (**Table 2**).
284
285 The number of predicted tRNA genes ranged from 76-197, the total number of protein-coding
286 genes predicted ranged from 9,029-10,920, and secondary metabolite cluster counts ranged from
287 15-27, 27 resulting from JES_112.
288
289
290
291 *Mating type loci determination*
292 The mating types were determined using prior work on members of Chaetothyriales and
293 Dothideomycetes including *Exophiala dermatitidis*, and *Aureobasidium pullulans* (Metin et al.
294 2019; Teixeira et al. 2017). Using collected nucleotide and protein FASTA sequences, BLAST
295 was used to identify the genes found in these loci. The genes in this locus are generally flanked by
296 SLA2 and APN2 and may sometimes have alternative genes within. **Figure 2** was generated using
297 JES_112, *Exophiala aquamarina* CBS 119918, *E. dermatitidis* NIH/UT8656, *E. dermatitidis* CBS

298 115663*,* and *Capronia coronata* CBS 617.96. The MAT locus is flanked by two genes, SLA2
299 (purple) and APN2 (orange). The MAT 1-1 gene, MAT 1-1-4 (green), and MAT 1-1-1 (teal) are
300 observed in *E. dermatitidis* CBS 115663 and *Capronia coronata*, while *E. dermatitidis*
301 NIH/UT8656 contains MAT 1-2 (pink) as does *Capronia coronata*. Our organism in question,
302 *Neophaeococcomyces mojaviensis* contains the MAT 1-2 gene along with the MAT 1-1-1 gene.
303 This is similarly seen with *N. aloes* FJII-L3-CM-P2. This is confusing as the MAT 1-1-1 gene
304 usually pairs with MAT 1-1-4. The gene arrow in blue is indicated as an L-type calcium channel
305 domain, while the gene in yellow is an unidentified functional gene or domain.
306
307 **Figure 3** was generated using JES_115 and JES_119 and two other species including,
308 *Aureobasidium pullulans* EXF-150 and *Coniosporium apollinis* CBS 100218. All species
309 described here only have the MAT 1-2 gene. The MAT locus is flanked by two genes, SLA2
310 (purple) and APN2 (orange). *Dothideomycetes* mating type loci look very different from the
311 *Chaetothyriales* mating type loci. Other genes included in this locus concern only a single MAT
312 locus, MAT 1-2 (pink), and rRNA adenine demethylase (yellow). Certain genes like the AP
313 endonuclease (teal) and a hypothetical protein (blue) are not seen in all four genomes.
314
315 *MCF morphology*
316 Strains showed limited and slow growth with black colonies on all media tested. Strain JES_119
317 produced abundant unilateral, hyaline budding cells which soon inflated, developed cruciate
318 septation, and became melanized. Strain JES_115 was hyphal with lateral chains of swollen cells
319 which occasionally detached. Strain JES_112 lacked sporulation, the thallus consisting of
320 melanized densely septate hyphae with series of somewhat inflated cells

321
322 During the annotation step, we processed the genomes through antiSMASH (**Table 3**), to detect
323 Biosynthetic Gene Clusters (BGCs) of secondary metabolites from the annotated genome
324 sequence. Once predicted metabolite of note, beta-lactone was found in all three MCF. A further
325 literature search indicates the importance of beta-lactone in industry as there have been multiple
326 products derived from these chemicals including, antifungals and anti-cancer agents (Robinson et
327 al. 2019). A BLASTP search of the JES_112 beta-lactone gene identified homologs to Acetyl-
328 CoA synthetase + 2-isopropylmalate synthases + bile acid dehydrogenase, zinc-binding alcohol
329 dehydrogenase + acetoacetate-CoA + NAD-dependent alcohol dehydrogenase, and AMP-binding
330 protein + 2-isopropylmalate synthases.
331
332 A second predicted metabolite of note was the siderophore gene cluster. These genes are involved
333 in iron transport, is a more well-known metabolite that could provide the organism with virulence
334 and protection by sequestering iron molecules from its surrounding environment (Johnson 2008;
335 Sass et al. 2019) and was primarily detected in JES_112.
336
337 Additionally, the BSC search revealed fungal-RiPPs (Ribosomal and post-transcriptionally
338 modified proteins) in JES_119. The homolog was best classified as a gamma-glutamyltransferase
339 + cytochrome protein. Fungal-RiPPs have been used as an alternative source of bioactive
340 metabolites and could be of industrial interest (Vogt and Künzler 2019). Additional BGCs were
341 found including Type-1 Polyketide synthases (T1PKS), Type-3 Polyketide synthases, non-
342 ribosomal peptide synthases, non-ribosomal peptide synthase-like, and terpenes.
343
344

345 *Four-locus gene trees*

346 The multi-gene internal-transcribed space (ITS1), large ribosomal subunit (LSU) beta-tubulin,
347 calmodulin tree (**Figure 4** and **Figure 5)** places the new isolates in context of named species in
348 the known genera (**Table 3**).

349 Forty-three isolates were used, and the alignment of the sequences were trimmed, and concatenated
350 to run the IQTree program and generate a concise multi-loci gene tree for *Neophaeococcomyces*
351 *mojaviensis* JES112. Here this strain is placed in the genus *Neophaeococcomyces*, along with
352 *Exophiala dermatitidis* NIH/UT8656, *E. radicis* P2854, *E. oligospoerma* CBS 265.49, *E.*
353 *oligospoerma* CBS 127587, and *E. xenobiotica* CBS 11817, *Fonsecaea pedrosoi* CBS 271.37,
354 *Capronia coronata* CBS 617.96, *Cladophialophora immunda* CBS 834.96, *C. carrionii* CBS
355 260.83, *C. yegresii* CBS 114405, *Neophaeococcomyces aloes* FIJI-L3-CM-P2*, N. catenatus*
356 CBS650.76*, N. oklahomaensis* EMSL 3313*, Knufia petricola* MA5789*, K. separata*
357 CGMCC3.17337*, K. mediterranea* CCFEE 6211*, K. mediterranea* CCFEE6205*, Knufia* sp. MV-
358 2018-MLT-8*, K. walvisbayicola* CBS 146989*, K. tsunedae* FMR10621*, Bradymyces yunnanensis*
359 CGmCC3.17350*, B. alpinus* CCFEE 5493*, Strelitziana africana* ICMP 21758 and ICMP 21760*,*
360 and *Tuber melanosporum* Mel8 as the outgroup.

361

362 The third phylogenetic tree, **Figure 5**, uses the same method described above as in **Figure 4**. 25
363 strains of Dothideomycetes MCF were included to place JES_115 and JES_119 into their proper
364 clades. MCF strains included a collection of *Coniosporium apollinis* CBS 100218*,* CBS 352.97*,*
365 *Aureobasidium mangrovei* IBRCM30265*, Aureobasidium* sp. AWRI4619-CO-2020*, Zalaria*
366 *obscura* FKI-L7-BK-DRAB2*, Polyplosphaeria fusca* CBS 125425*, Leptosphaeria maculans* JN3*,*

367 *Leptosphaeria biglobosa* CA1*, Phaeosphaeria* sp. MPI-PUGE-AT-0046c*, Alternaria solani*
368 NL03003*, Cenococcum geophilum* 1.58*, Venturia pyrina* ICMP11032*, Coniosporium uncinatum*
369 CBS 100219*,* and CCFEE 6149, *Scorias spongiosa* HLSS1*, Polychaeton citri* CBS 116435*,*
370 *Zymoseptoria tritici* CBS 100329*, Neohortaea acidophila* CBS 113389*, Salinomyces thailandica*
371 CCFEE 6315*, Hortaea werneckii* EXF-2000*, Baudoinia panamericana* UAMH 10762*,*
372 *Teratosphaeria guachensis* CMW 17545*, Friedmanniomyces simplex* CCFEE 5184*,*
373 *Friedmanniomyces endolithicus* CCFEE 5311*,* and *Tuber melanosporum* Mel8 as the outgroup.
374 JES_115 groups near *Coniosporium* spp.*, w*hile JES_119 groups near *Aureobasidium* spp.
375
376 *Taxonomy*
377 ***Neophaococcomyces mojaviensis sp. nov.*, Kurbessoian, Ahmed, de Hoog and Stajich -**
378 **Mycobank (848161). Description:** Colonies on MEA, OA, PDA after two weeks of incubation at
379 25°C attain diameters of 1.6, 2, 2.2, and 1.6 mm respectively. Hyphae 2.9-5.4 µm diameter, dark
380 brown or black, smooth or occasionally rough walled, cells eventually inflating up to 8 µm in
381 diameter. The proliferation of inflated cells might result in the formation of multicellular bodies
382 terminal or intercalary in the hyphae measuring 13.8-31.8 µm, multiseptate with transverse and
383 longitudinal septa; bodies round or irregular, dark brown to black and thick-walled. No conidia
384 were observed. Sexual state unknown.
385 **Holotype:** ATCC (TSD-444), preserved at the herbarium collection of the Westerdijk Fungal
386 Biodiversity Institute, Utrecht, The Netherlands. Living culture ex-type ATCC (TSD-444).
387 **Diagnosis:** Strain JES_112 clusters in the order *Chaetothyriales*, relatively close to the numerous
388 rock-inhabiting species of the genus *Knufia*, and amidst the species of the small genus

389 *Neophaeococcomyces*. Both genera are assigned to the family *Trichomeriaceae*, containing 'sooty
390 molds' with oligotrophic lifestyles colonizing inert surfaces (Chomnunti et al. 2012). The cluster
391 *Neophaeococcomyces,* based on *N. catenatus* as generic type species, as yet contains only four
392 species, which mostly were isolated from low nutrient habitats, such as the bark of *Aloe*, stone, or
393 air. Several species of the genus show budding with melanized cells, and frequently cells cohere
394 in short chains. Often lateral branches of short inflated cells are inserted on hyphae; the cells may
395 be released as arthroconidia which then swell or appear yeast-like, or remain coherent.
396
397 ***Coniosporium tulheliwenetii sp. nov*., Kurbessoian, Ahmed, de Hoog and Stajich - MycoBank**
398 **(848162).**
399 **Description:** Colonies on MEA, OA, PDA, after 2 weeks of incubation at 25°C attain diameter
400 restricted, measuring 1.1 cm, 0.72 cm, and 0.75cm, respectively. Hyphae 4.6-8.4 µm diameter
401 showing lateral chains of swollen cells 7.7 - 10.8 µm. The cells however remain intact, and no
402 conidia was observed. Teleomorph unknown.
403 **Holotype: CBS (150075), and herbarium CBS H-25288**, preserved at the herbarium collection
404 of the Westerdijk Fungal Biodiversity Institute, Utrecht, The Netherlands. Living culture ex-type
405 CBS (150075).
406 **Diagnosis:** Strain JES_115 was morphologically similar to *Knufia* species in the presence of lateral
407 chains of swollen cells inserted on main hyphae, the cells eventually being released as conidia, but
408 was phylogenetically remote. It clustered with some species of rock-inhabiting described in
409 *Coniosporium,* in the order *Pleosporales*. Interestingly, the original descriptions, which were made
410 before sequence data were available, classified them all into a single genus. The genus

411 *Coniosporium* is one of the classical genera of meristematic fungi. However, most species were
412 described in the 19th century, including the generic type species *C. olivaceum*, and voucher
413 specimens are lost. Nevertheless, Haridas et al. (2020) introduced the family *Coniosporiaceae* and
414 order *Coniosporales* using the few recently described rock-inhabiting fungi, *C. apollinis* and *C.*
415 *uncinatum* as reference (Haridas et al. 2020). It should be noted that the family *Coniosporiaceae*
416 was already used by Nannfeldt for the genus *Coniospora*.
417
418 ***Taxawa* gen. nov. Kurbessoian, Ahmed, de Hoog and Stajich - MycoBank (848163).**
419 Type species: *Taxawa tesnikishii*
420 *Taxawa tesnikishii sp. nov.* Kurbessoian, Ahmed, de Hoog and Stajich - MycoBank (848164).
421 **Description:** Colonies moist, black, regular and flat on OA and heaped irregular on MEA and
422 PDA, measuring 1.4-1.8 cm in diameter growing on MEA, OA, and PDA at 25°C . Hyphae
423 smooth, thick-walled, measuring 6.1-10.3 µm wide. Yeast cells abundant produce unilateral
424 budding 2.7-4.8 µm, subsequently inflating and becoming crucially septate and melanized with
425 age. Clusters of black meristematic bodies (9.0-56.8 µm) were observed. Sexual state unknown.
426 **Holotype: CBS (150074), and herbarium CBS H-25287**, preserved at the herbarium collection
427 of the Westerdijk Fungal Biodiversity Institute, Utrecht, The Netherlands. Living culture ex-type
428 CBS (150074).
429 **Diagnosis:** Strain JES_119 showed similar morphology to the cultural states of e.g. *Sydowia* and
430 *Comminutispora*, and has been described in the asexual genus *Phaeotheca*. Thambugala et al.
431 (2014) erected the family *Aureobasidiaceae* for fungi in this relationship, but also this name
432 existed already, *Aureobasidiaceae* Ciferri (1958) (Thambugala et al. 2014), based on the same

433 species, *Aureobasidium pullulans* (Ciferri 1958). Only a small number of extant species has been
434 sequenced, and the genome trees show an even larger taxon sampling effect, but given our current
435 inability to assign strain JES_119 to any genus, we introduce the genus *Taxawa*.
436
437 **Discussion**
438
439 BSCs are an untapped resource of novel microorganisms, using non-traditional methods of
440 culturing may be a method to uncover more unavailable species for sequencing. Using a pour plate
441 method for culturing allows the microorganism to avoid complete oxygen saturation (or oxygen
442 toxicity), and instead can grow in low to micro-aerophilic concentrations of oxygen (Stevens
443 1995). Collecting MCF using this method has proved to be efficient, as fast-growing fungi
444 overtake the surface of plates, while MCF can tolerate lower oxygen concentrations, thus
445 localizing to the bottom of plates. Preparing axenic cultures of MCF is then relatively easy and
446 can also increase the rate of isolation as MCF tends to take two weeks to grow. A hypothesis about
447 the facultative aerobic or microaerophilic nature of MCF could also be seen in the phenotype of
448 these species. Morphological growth on surface of petri plates shows unusual furrowing and
449 clumping growth (JES_119, JES_115), some strains (JES_112) grow underneath the surface of the
450 plate which seem to be MCF adaptations to the high concentration of oxygen present on petri
451 plates.
452
453 The high melanin content of MCF complicates efforts to extract high molecular weight (HMW)
454 DNA for sequencing, however adjustments to standard fungal CTAB can dramatically improve
455 the gDNA purity. In the case for these BSC MCF, an increase in phenol:chloroform and
456 chloroform washes allow for melanin to be removed completely from the DNA samples. Another

457 consideration to help concentrate more DNA is to incubate the DNA sample in -20°C overnight
458 during the DNA precipitation step. Using long read sequencing technology (Oxford ONT) it is
459 best to have a very high concentration of clean DNA to process and thus could be the limiting
460 factor for these sequencing procedures. Using hybrid methods of sequencing (Illumina and
461 Nanopore) provides scientists the proper backbone to develop *de-novo* assemblies (Stevens 1995;
462 Khezri et al. 2021; Chen et al. 2020; Saud et al. 2021). It is vital to have as near complete
463 assemblies of species as possible, this provides the scientific community with the best tools for
464 proper genomic assessments. For future research endeavors, a second nanopore flow cell would
465 be necessary to help build a better assembly for strain JES_112 (*Neophaeococcomyces*
466 *mojaviensis*) as the telomere analysis failed on this first round of assembly. The other two strains
467 had enough depth of coverage that allowed for different programs to optimize the assembly and
468 have more closed telomere contigs.
469
470 Scientific literature describing novel MCF always note the clonal or asexual nature, describing
471 "missing" sexual states and thus always being in a haploid state. The MAT locus is one of the
472 pivotal regions in the fungal genome that provides more accurate ploidy and sexual states of
473 fungi, and using this data to describe the three new MCF assisted in understanding the sexual
474 states. JES_115 and JES_119 as the two *Dothideomycetes* representatives indicate heterothallic
475 sexual states having only the MAT1-2 gene, *vs.* homothallic species having representatives of
476 both MAT1-1 and MAT1-2 genes. Better genome assembly would help better describe the
477 JES_112 MAT locus as there is the presence of MAT1-2 but also a portion of the MAT1-1 gene
478 (as it is composed of two genes, MAT1-1-1 and MAT1-1-4). The high melanin content of MCF

479 could prove to be difficult when testing for ploidy in the scientific "gold standard" method (flow
480 cytometry). But future research would most benefit from having this method optimized to
481 understand not only the new MCF described in this work but also for future MCF considerations.
482 Possibly the sexual states have not yet been described or seen for MCFs and may require a
483 particular environmental stimulus to produce the proper structures to reproduce. Possibly, other
484 forms of propagation are found in other habitats. A prototypical example is *Auerobasidium*
485 *pullulans* which shows meristematic growth on glass or rock but is a rapidly expanding yeast-
486 like fungus in culture. There has also been an increase in literature describing clonal MCF having
487 high hybridization rates that create pseudo but stable diploids without the process of
488 recombination (Gostinčar et al. 2022). This was not detected in these three species described in
489 this paper.
490
491 MCF morphology indicates usual slow growth (about two weeks) seen in most MCF described
492 previously (Selbmann et al. 2014; Chowdhary et al. 2014; Hölker et al. 2004; Zhao et al. 2010;
493 Kejžar et al. 2013). JES_119, as it develops over time, increases its melanin production and
494 develops from a bright orange-yellow color to a more deeply pigmented black. The budding cells
495 are unilateral and are uncommon in other described MCF, and it was evaluated as a previously
496 undescribed genus and species in Class *Dothideomycetes* as *Taxawa tesnikishii.* Strain JES_115
497 has a phenotype that is commonly seen in MCF, but due to its complicated taxonomy history, the
498 genus *Coniosporium* remains as a genus of doubtful identity. The species JES_112 is one of the
499 few described *Neophaeococcomyces* available anywhere and thus an important contribution to the
500 scientific community.
501

502 Finding MCF from extreme environments such as BSCs may point to harbored secondary
503 metabolites either absorbed from surrounding species through horizontal gene transfer (HGT) or
504 adapted from time. MCF are known to use secondary metabolites to help survive such extremes
505 and are thus an untapped resource for the identification of novel metabolites. An example to be
506 described by Dr. Erin Carr, *Neophaeococcomyces* sp, has been shown to have an obligate bacterial
507 hitchhiker (Carr 2022). JES_115 and JES_119 both contain about 15 secondary metabolites
508 detected by antiSMASH, which is a considerable number when compared to other fungi (Rateb
509 and Ebel 2011). The roles of secondary metabolites in modern human industry applications are
510 vast (Demain 2014) and thus would be important to test and compare across all MCF.

511

512 **Conclusions**

513

514 Biological soil crusts are an untapped resource for novel microorganisms as evidenced by our
515 work. The MCF we collected are incredibly slow growing and could be easily missed during
516 culturing attempts. The method described here (and detailed in **Appendix 1**) improved the chances
517 for isolation of these species. MCFs have been isolated from different types of extreme
518 environments including BSC's.

519

520 An interesting consideration for species JES_112 or *Neophaeococcomyces mojaviensis* is through
521 personal communications with another MCF scientist, Erin Carr, who also isolated a species of
522 *Neophaococcomyces*, named "Crusty" from a biological soil crust. Their species was associated
523 with a pink *Methylobacterium* symbiont, which she calls "Light Pinky"and "Dark Pinky". Her
524 assessment of this symbiosis suggests the role of the symbiont is involved in aerobic anoxygenic
525 photosynthesis and auxin production (Carr 2022). Through our multiple culturing attempts, there

was no indication of a pink symbiont, but the possible bacteria signal within our secondary metabolite assessment could be attributed to a contamination from this bacterium. JES_112 will be the second known genome of the genus *Neophaeococcomyces* found in GenBank as JAPDRQ000000000.

Species JES_119 or *Taxawa tesnikishi* is the first isolated of this phenotype. This species was closer to *Aureobasidium*, yet phenotypically is very different from identified *Aureobasidium* species. Using fungal phenotype and phylogenomics, we were able to determine the microorganism is different from known *Aureobasidium* species and may be of a new genus, hence the naming *Taxawa* as its genus name. *Taxawa tesnikishi* is the first known genus and species, now available in Genbank as JAPDRO000000000.

Species JES_115 or *Coniosporium tulheliwenetii* was also collected from the BSC's from Boyd Deep Canyon and was thus honored with a Cahuilla term used to describe BSC phenotypic features seen on the soil. The genus *Coniosporium* has historically been confusing, as the earliest strains were collected in the late 1800s. Initial collections of *Coniosporium* were placed in Chaetothyriales, while later similar MCF phenotypes were also grouped with *Coniosporium*, to be later considered as Dothideomycetes instead. A careful reorganization and assessment of the genus is desperately needed. Genome assembly is now available as JAPDRP000000000.

Acknowledgments

This work was performed in part at the University of California Natural Reserve System (Boyd Deep Canyon Desert Research Center) Reserve DOI: (doi:10.21973/N3V66D) (UCNRS Information Manager 1965) and at Joshua Tree National Park under permits generated through the help and guidance of Nuttapon Pombubpa, permit numbers: JOTR-2015-SCI-0033, JOTR-

2016-SCI-0036, JOTR-2017-SCI-0044, JOTR-2018-SCI-0035, JOTR-2019-SCI-0031. Many thanks to Nicole Pietrasiak for her extensive knowledge in biological soil crusts. Many thanks also to Joshua Tree Reserve members who helped facilitate the admission of our Joshua Tree sample, specifically Anna R Tegarden, Ann Hitchcock, and Jay Goodwin.

Funding

T.K was partially supported by NIH grant R01 AI127548 (support to J.E.S. via Deborah Hogan). Computational analyses were performed at the University of California – Riverside HPCC, supported by grants from the National Science Foundation (DBI – 1429826 and 2215705) and NIH (S10OD016290). JES is a CIFAR Fellow in the Fungal Kingdom: Threats and Opportunities program.

Figure Legends:

Figure 1. Microscopic morphology of isolated MCF. (1) *Taxawa tesnikishii* JES_119, colonies on MEA (A), OA (B), and PDA (C) agars, meristematic cells (D-F), and budding cells (G-M); (2) *Coniosporium tulheliwenetii* JES_115, colonies on MEA (A), OA (B), and PDA (C) agars, hyphae with lateral branches of swollen cells reluctantly leading to arthroconidia (D-J); (3) *Neophaeococcomyces mojaviensis* JES_112, colonies on MEA (A), OA (B), and PDA (C) agars, hyphae producing intercalary swollen cells without conidiation (D-J). Microscopic mounts were made in lactic acid and examined using a light microscope. The scale depicted here is 25µm.

Figure 2. Mating type loci determined for Chaetothyriales JES_112 here called *Neophaeococcomyces mojaviensis.* Other MCFs added to this analysis include *Neophaeococcomyces aloes* FJII-L3-CM-P2, *Exophiala dermatitidis* NIH/UT8656, *E. dermatitidis* CBS 115663, and *Capronia coronata* CBS 617.96. The MAT locus is flanked by two genes, SLA2 (purple) and APN2 (orange). The MAT 1-1 gene, MAT 1-1-4 (green), and MAT 1-1-1 (teal) are observed in *E. dermatitidis* CBS 115663 and *C. coronata*, while *N. aloes* and *E. dermatitidis* NIH/UT8656 contain MAT 1-2 (pink) as does *C. coronata*. Our organism in question, *N. mojaviensis* contains the MAT 1-2 and MAT 1-1-1 gene which is confusing as it is not common to lose the MAT 1-1-4. The gene arrow in blue is indicated as an L-type calcium channel domain, while the gene in yellow is an unidentified functional gene or domain.

Figure 3. Mating type loci determined for Dothideomycetes JES_115 and JES_119, here called *Coniosporium tulheliwenetii* and *Taxawa tesnikishi*. Other dothideaceous black yeast-like fungi in this

586 analysis include *Aureobasidium pullulans* EXF-150, and *Coniosporium apollinis CBS* 100218. All species
587 described here only have the MAT 1-2 gene. The MAT locus is flanked by two genes, SLA2 (purple) and
588 APN2 (orange). *Dothideomycetes* mating type loci look very different from the *Chaetothyriales* mating
589 type loci. Other genes included in this locus include only a single MAT locus, MAT 1-2 (pink). Another
590 gene included in this locus is rRNA adenine demethylase (yellow). Certain genes like the AP endonuclease
591 (teal) and a hypothetical protein (blue) are not seen in all four genomes.
592
593 **Figure 4. Chaetothyriales multi-locus gene tree.** Multi-loci phylogenetic tree using 4 highly conserved
594 genes including, beta-tubulin, calmodulin, internal-transcribed sequence (ITS), and the large subunit of
595 the Ribosome (LSU). Seven representative strains with loci were used, which were aligned, trimmed, and
596 concatenated to run the IQTree program and generate a concise multi-loci gene tree for
597 *Neophaeococcomyces mojaviensis* JES112. Here this strain is placed in the *Neophaeococcomyces* genera.
598
599 **Figure 5. Dothideomycetes multi-locus gene tree.** Multi-loci phylogenetic tree using 4 highly
600 conserved genes including, beta-tubulin, calmodulin, internal-transcribed sequence (ITS), and the large
601 subunit of the Ribosome (LSU). Twenty-five representative strains with loci were used, which were
602 aligned, trimmed, and concatenated to run the IQTree program and generate a concise multi-loci gene tree
603 for JES_115 and JES_119 or *Coniosporium tulheliwenetii* and *Taxawa tesnikishii* respectively. Here
604 strain JES_115 is grouping with other *Coniosporium* spp., while JES_119 is grouping with but distinctly
605 apart from *Aureobasidium* spp.
606
607 **Table 1. Three species were collected from biological soil crusts collected from two desert locations**
608 **in Southern California.** Strain JES_112 was isolated from the south east region of Joshua Tree National
609 Park in the Mojave Desert, while JES_115 and JES_119 were both collected from biological soil crusts
610 collected from the campground site in the UC Natural Reserve of Boyd Deep Canyon.
611
612 **Table 2. Genome assembly and annotation summary statistics.** All strains were sequenced with
613 Illumina and Nanopore sequencing. With the added sequencing reads, we were able to glean telomere
614 information along with genome completeness. It is clear that JES_112 initially is contaminated as the
615 BUSCO score is lower, while JES_115 and JES_119 are much closer to a more complete genome.
616
617 **Table 3. Predicted secondary metabolite gene clusters.** The BGCs predicted include multiple copies of
618 PKS and NRPS genes, but siderophores were only recovered in JES_112. There was a higher number of
619 BGCs predicted in JES_112 (27) our *Chaetothyriales* species, than JES_115 and JES_119 (15) our
620 *Dothideomycetes*. This table lists the numbers of each. JES_112 has a much higher number (27) of
621 secondary metabolites than the other two (15).
622
623 **Table 4. Gene Tree Nucleotide Accession numbers.** Collected accession numbers of alternative strains
624 to build Figures 4 and 5. The remaining empty spaces indicate the need to pull the sequences using BLAST.
625 Once collected each gene populated a gene FASTA file, aligned, clipped and IQTREE2, a tree-building
626 program, was run to determine the gene models for each gene. Once determined, the gene alignment lengths
627 were calculated and partitioning scripts were described and used to build a larger tree, using IQTREE2.
628
629

References:

Bankevich A, Nurk S, Antipov D, Gurevich AA, Dvorkin M, Kulikov AS, Lesin VM, Nikolenko SI, Pham S, Prjibelski AD, et al. 2012. SPAdes: a new genome assembly algorithm and its applications to single-cell sequencing. J Comput Biol. 19(5):455–477.

Bell AA, Wheeler MH. 1986. Biosynthesis and Functions of Fungal Melanins. Annu Rev Phytopathol. 24(1):411–451.

Belnap J, Harper KT. 1995. Influence of cryptobiotic soil crusts on elemental content of tissue of two desert seed plants. Arid Soil Research and Rehabilitation. 9(2):107–115.

Beraldi-Campesi H, Retallack GJ. 2016b. Terrestrial Ecosystems in the Precambrian. In: Weber B, Büdel B, Belnap J, editors. Biological Soil Crusts: An Organizing Principle in Drylands. Cham: Springer International Publishing. p. 37–54.

Blin K, Shaw S, Kloosterman AM, Charlop-Powers Z, van Wezel GP, Medema MH, Weber T. 2021. antiSMASH 6.0: improving cluster detection and comparison capabilities. Nucleic Acids Res. 49(W1):W29–W35.

Brown J, Boyd J. 1922. History of San Bernardino and Riverside Counties: With Selected Biography of Actors and Witnesses of the Period of Growth and Achievement. Western Historical Association.

Brůna T, Lomsadze A, Borodovsky M. 2020. GeneMark-EP : eukaryotic gene prediction with self-training in the space of genes and proteins. NAR Genomics and Bioinformatics. 2(2). doi:10.1093/nargab/lqaa026. http://dx.doi.org/10.1093/nargab/lqaa026.

Bushnell B. 2014. BBMap: A fast, accurate, splice-aware aligner. Lawrence Berkeley National Lab. (LBNL), Berkeley, CA (United States) Report No.: LBNL-7065E. https://www.osti.gov/biblio/1241166.

Carr EC. 2022. Discovering Novel Polyextremotolerant Fungi, and Determining Their Ecological Role Within the Biological Soil Crust Consortium.

Casadevall A, Rosas AL, Nosanchuk JD. 2000. Melanin and virulence in *Cryptococcus neoformans*. Current Opinion in Microbiology. 3(4):354–358. doi:10.1016/s1369-5274(00)00103-x.

Casadevall A, Steenbergen JN, Nosanchuk JD. 2003. “Ready made” virulence and “dual use” virulence factors in pathogenic environmental fungi — the *Cryptococcus neoformans* paradigm. Current Opinion in Microbiology. 6(4):332–337. doi:10.1016/s1369-5274(03)00082-1.

Chomnunti P, Bhat DJ, Jones EBG, Chukeatirote E, Bahkali AH, Hyde KD. 2012. Trichomeriaceae, a new sooty mould family of Chaetothyriales. Fungal Divers. 56(1):63–76.

673 Chowdhary A, Perfect J, de Hoog GS. 2014. Black Molds and Melanized Yeasts Pathogenic to Humans.
674 Cold Spring Harb Perspect Med. 5(8):a019570.
675
676 Ciferri R. 1958. Affinity between fungi of the verrucous dermatitis and sooty-molds. Mycopathol Mycol
677 Appl. 9(3):197–200.
678
679 Cock PJA, Antao T, Chang JT, Chapman BA, Cox CJ, Dalke A, Friedberg I, Hamelryck T, Kauff F,
680 Wilczynski B, et al. 2009. Biopython: freely available Python tools for computational molecular biology
681 and bioinformatics. Bioinformatics. 25(11):1422–1423.
682
683 Dadachova E, Bryan RA, Howell RC, Schweitzer AD, Aisen P, Nosanchuk JD, Casadevall A. 2008. The
684 radioprotective properties of fungal melanin are a function of its chemical composition, stable radical
685 presence and spatial arrangement. Pigment Cell Melanoma Res. 21(2):192–199.
686
687 Dadachova E, Casadevall A. 2008. Ionizing radiation: how fungi cope, adapt, and exploit with the help of
688 melanin. Curr Opin Microbiol. 11(6):525–531.
689
690 Demain AL. 2014. Valuable Secondary Metabolites from Fungi. In: Martín J-F, García-Estrada C,
691 Zeilinger S, editors. Biosynthesis and Molecular Genetics of Fungal Secondary Metabolites. New York,
692 NY: Springer New York. p. 1–15.
693
694 Evans RD, Ehleringer JR. 1993. A break in the nitrogen cycle in aridlands? Evidence from δp15N of
695 soils. Oecologia. 94(3):314–317.
696
697 Finn RD, Bateman A, Clements J, Coggill P, Eberhardt RY, Eddy SR, Heger A, Hetherington K, Holm L,
698 Mistry J, et al. 2014. Pfam: the protein families database. Nucleic Acids Res. 42(Database issue):D222–
699 30.
700
701 Gilchrist CLM, Chooi Y-H. 2021 Jan 18. Clinker & clustermap.js: Automatic generation of gene cluster
702 comparison figures. Bioinformatics. doi:10.1093/bioinformatics/btab007.
703
704 Gómez BL, Nosanchuk JD. 2003. Melanin and fungi. Curr Opin Infect Dis. 16(2):91–96.
705
706 Gorbushina AA, Whitehead K, Dornieden T, Niesse A, Schulte A, Hedges JI. 2003. Black fungal
707 colonies as units of survival: hyphal mycosporines synthesized by rock-dwelling microcolonial fungi. Can
708 J Bot. 81(2):131–138.
709
710 Gostinčar C, Sun X, Černoša A, Fang C, Gunde-Cimerman N, Song Z. 2022. Clonality, inbreeding, and
711 hybridization in two extremotolerant black yeasts. Gigascience. 11. doi:10.1093/gigascience/giac095.
712
713 Green TGA, Allan Green TG, Proctor MCF. 2016. Physiology of Photosynthetic Organisms Within
714 Biological Soil Crusts: Their Adaptation, Flexibility, and Plasticity. Biological Soil Crusts: An
715 Organizing Principle in Drylands.:347–381. doi:10.1007/978-3-319-30214-0_18.
716

Green TGA, Broady PA. 2001. Biological soil crusts of Antarctica. In: Ecological Studies. Berlin, Heidelberg: Springer Berlin Heidelberg. (Ecological studies: analysis and synthesis. Berlin, Heidelberg, New York NY). p. 133–139.

Gümral R, Tümgör A, Saraçlı MA, Yıldıran ŞT, Ilkit M, de Hoog GS. 2014. Black yeast diversity on creosoted railway sleepers changes with ambient climatic conditions. Microb Ecol. 68(4):699–707.

Haas BJ, Salzberg SL, Zhu W, Pertea M, Allen JE, Orvis J, White O, Buell CR, Wortman JR. 2008. Automated eukaryotic gene structure annotation using EVidenceModeler and the Program to Assemble Spliced Alignments. Genome Biol. 9(1):R7.

Haridas S, Albert R, Binder M, Bloem J, LaButti K, Salamov A, Andreopoulos B, Baker SE, Barry K, Bills G, et al. 2020. 101 Dothideomycetes genomes: A test case for predicting lifestyles and emergence of pathogens. Stud Mycol. 96:141–153.

Hölker U, Bend J, Pracht R, Tetsch L, Müller T, Höfer M, de Hoog GS. 2004. *Hortaea acidophila*, a new acid-tolerant black yeast from lignite. Antonie Van Leeuwenhoek. 86(4):287–294.

de Hoog GS, Hermanides-Nijhof EJ. 1977. The Black Yeasts and Allied Hyphomycetes, Studies in Mycology. Baarn, The Netherlands: Centraalbureau voor Schimmelcultures.

de Hoog GS, Matos T, Sudhadham M, Luijsterburg KF, Haase G. 2005. Intestinal prevalence of the neurotropic black yeast *Exophiala (Wangiella) dermatitidis* in healthy and impaired individuals. Mycoses. 48(2):142–145.

Hoog GS de, Queiroz-Telles F, Haase G, Fernandez-Zeppenfeldt G, Angelis DA, H. G. Gerrits van den Ende A, Matos T, Peltroche-Llacsahuanga H, Pizzirani-Kleiner AA, Rainer J, et al. 2000a. Black fungi: clinical and pathogenic approaches. Med Mycol. 38(sup1):243–250.

Hooper L. 1920. The Cahuilla Indians. University of California Press.

Housman DC, Yeager CM, Darby BJ, Sanford RL, Kuske CR, Neher DA, Belnap J. 2007. Heterogeneity of soil nutrients and subsurface biota in a dryland ecosystem. Soil Biol Biochem. 39(8):2138–2149.

Huerta-Cepas J, Szklarczyk D, Heller D, Hernández-Plaza A, Forslund SK, Cook H, Mende DR, Letunic I, Rattei T, Jensen LJ, et al. 2019. eggNOG 5.0: a hierarchical, functionally and phylogenetically annotated orthology resource based on 5090 organisms and 2502 viruses. Nucleic Acids Res. 47(D1):D309–D314.

James TY, Stajich JE, Hittinger CT, Rokas A. 2020. Toward a Fully Resolved Fungal Tree of Life. Annu Rev Microbiol. 74:291–313.

Johnson L. 2008. Iron and siderophores in fungal–host interactions. Mycol Res. 112(2):170–183.

Jones P, Binns D, Chang H-Y, Fraser M, Li W, McAnulla C, McWilliam H, Maslen J, Mitchell A, Nuka G, et al. 2014. InterProScan 5: genome-scale protein function classification. Bioinformatics. 30(9):1236–1240.

Kejžar A, Gobec S, Plemenitaš A, Lenassi M. 2013. Melanin is crucial for growth of the black yeast *Hortaea werneckii* in its natural hypersaline environment. Fungal Biology. 117(5):368–379. doi:10.1016/j.funbio.2013.03.006. http://dx.doi.org/10.1016/j.funbio.2013.03.006.

Korf I. 2004. Gene finding in novel genomes. BMC Bioinformatics. 5:59.

Kroeber AL. 1925. Handbook of the Indians of California. U.S. Government Printing Office.

Kurbessoian T. 2022. tania-k/Chapter2.3MCF: V1. https://zenodo.org/record/7259500.

Lal R. 2004b. Carbon sequestration in dryland ecosystems. Environ Manage. 33(4):528–544.

Lanfear R, Calcott B, Kainer D, Mayer C, Stamatakis A. 2014. Selecting optimal partitioning schemes for phylogenomic datasets. BMC Evol Biol. 14:82.

Little AEF, Currie CR. 2008. Black yeast symbionts compromise the efficiency of antibiotic defenses in fungus-growing ants. Ecology. 89(5):1216–1222.

Lowe TM, Chan PP. 2016. tRNAscan-SE On-line: integrating search and context for analysis of transfer RNA genes. Nucleic Acids Res. 44(W1):W54–7.

Maestre FT, Soliveres S, Gotelli NJ, Quero JL, Berdugo M. 2012. Response to Comment on “Plant Species Richness and Ecosystem Multifunctionality in Global Drylands.” Science. 337(6091):155–155. doi:10.1126/science.1220620. http://dx.doi.org/10.1126/science.1220620.

Majoros WH, Pertea M, Salzberg SL. 2004. TigrScan and GlimmerHMM: two open source ab initio eukaryotic gene-finders. Bioinformatics. 20(16):2878–2879.

Manni M, Berkeley MR, Seppey M, Simão FA, Zdobnov EM. 2021. BUSCO Update: Novel and Streamlined Workflows along with Broader and Deeper Phylogenetic Coverage for Scoring of Eukaryotic, Prokaryotic, and Viral Genomes. Mol Biol Evol. 38(10):4647–4654.

Mehdiabadi NJ, Schultz TR. Natural history and phylogeny of the fungus-farming ants (Hymenoptera: Formicidae: Myrmicinae: Attini). [accessed 2022 Mar 29].

Metin B, Döğen A, Yıldırım E, de Hoog GS, Heitman J, Ilkit M. 2019. Mating type (MAT) locus and possible sexuality of the opportunistic pathogen *Exophiala dermatitidis*. Fungal Genetics and Biology. 124:29–38. doi:10.1016/j.fgb.2018.12.011.

Nosanchuk JD, Stark RE, Casadevall A. 2015. Fungal melanin: What do we know about structure? Front Microbiol. 6:1463.

Palmer JM, Stajich J. 2020. Funannotate v1.8.1: Eukaryotic genome annotation. https://zenodo.org/record/4054262.

Pietrasiak N. 2005. Field guide to classify biological soil crusts for ecological site evaluation. NRCS.

Pietrasiak N, Regus JU, Johansen JR, Lam D, Sachs JL, Santiago LS. 2013. Biological soil crust community types differ in key ecological functions. Soil Biol Biochem. 65:168–171.

Potter SC, Luciani A, Eddy SR, Park Y, Lopez R, Finn RD. 2018. HMMER web server: 2018 update. Nucleic Acids Res. 46(W1):W200–W204.

Rateb ME, Ebel R. 2011. Secondary metabolites of fungi from marine habitats. Nat Prod Rep. 28(2):290–344.

Rawlings ND, Barrett AJ, Thomas PD, Huang X, Bateman A, Finn RD. 2018. The MEROPS database of proteolytic enzymes, their substrates and inhibitors in 2017 and a comparison with peptidases in the PANTHER database. Nucleic Acids Res. 46(D1):D624–D632.

Revell LJ. 2012. phytools: an R package for phylogenetic comparative biology (and other things). Methods Ecol Evol. 3(2):217–223.

Robinson SL, Christenson JK, Wackett LP. 2019. Biosynthesis and chemical diversity of β-lactone natural products. Nat Prod Rep. 36(3):458–475.

Rozenstein O, Karnieli A. 2015. Identification and characterization of Biological Soil Crusts in a sand dune desert environment across Israel–Egypt border using LWIR emittance spectroscopy. J Arid Environ. 112:75–86.

Sass G, Ansari SR, Dietl A-M, Déziel E, Haas H, Stevens DA. 2019. Intermicrobial interaction: *Aspergillus fumigatus*siderophores protect against competition by *Pseudomonas aeruginosa*. PLoS One. 14(5):e0216085.

Saunte DM, Tarazooie B, Arendrup MC, de Hoog GS. 2012a. Black yeast-like fungi in skin and nail: it probably matters. Mycoses. 55(2):161–167.

Siletti CE, Zeiner CA, Bhatnagar JM. 2017. Distributions of fungal melanin across species and soils. Soil Biol Biochem. 113:285–293.

Slater GSC, Birney E. 2005. Automated generation of heuristics for biological sequence comparison. BMC Bioinformatics. 6:31.

SMIT A. F. A. 2004. Repeat-Masker Open-3.0. http://www.repeatmasker.org.

Sofi MY, Shafi A, Masoodi KZ. 2022. NCBI BLAST. Bioinformatics for Everyone.:95–102. doi:10.1016/b978-0-323-91128-3.00021-5.

Staley JT, Palmer F, Adams JB. 1982. Microcolonial fungi: common inhabitants on desert rocks? Science. 215(4536):1093–1095.

Stanke M, Keller O, Gunduz I, Hayes A, Waack S, Morgenstern B. 2006. AUGUSTUS: ab initio prediction of alternative transcripts. Nucleic Acids Res. 34(Web Server issue):W435–9.

Steenbergen JN, Casadevall A. 2003. The origin and maintenance of virulence for the human pathogenic fungus Cryptococcus neoformans. Microbes Infect. 5(7):667–675.

Stevens TO. 1995. Optimization of media for enumeration and isolation of aerobic heterotrophic bacteria from the deep terrestrial subsurface. J Microbiol Methods. 21(3):293–303.

Taborda CP, da Silva MB, Nosanchuk JD, Travassos LR. 2008b. Melanin as a virulence factor of Paracoccidioides brasiliensis and other dimorphic pathogenic fungi: a minireview. Mycopathologia. 165(4-5):331–339.

Teixeira MM, Moreno LF, Stielow BJ, Muszewska A, Hainaut M, Gonzaga L, Abouelleil A, Patané JSL, Priest M, Souza R, et al. 2017. Exploring the genomic diversity of black yeasts and relatives (Chaetothyriales, Ascomycota). Stud Mycol. 86:1–28.

Thambugala KM, Ariyawansa HA, Li Y-M, Boonmee S, Hongsanan S, Tian Q, Singtripop C, Bhat DJ, Camporesi E, Jayawardena R, et al. 2014. Dothideales. Fungal Divers. 68(1):105–158.

Thanh VN, Hien DD. 2019. *Moniliella floricola* sp. nov., a species of black yeast isolated from flowers. International Journal of Systematic and Evolutionary Microbiology. 69(1):87–92. doi:10.1099/ijsem.0.003099. http://dx.doi.org/10.1099/ijsem.0.003099.

UCNRS Information Manager. 1965. Boyd deep canyon desert research center. doi:10.21973/N3V66D.

Vicente VA, Attili-Angelis D, Pie MR, Queiroz-Telles F, Cruz LM, Najafzadeh MJ, de Hoog GS, Zhao J, Pizzirani-Kleiner A. 2008. Environmental isolation of black yeast-like fungi involved in human infection. Stud Mycol. 61:137–144.

Vogt E, Künzler M. 2019. Discovery of novel fungal RiPP biosynthetic pathways and their application for the development of peptide therapeutics. Appl Microbiol Biotechnol. 103(14):5567–5581.

Wang L-G, Lam TT-Y, Xu S, Dai Z, Zhou L, Feng T, Guo P, Dunn CW, Jones BR, Bradley T, et al. 2020. Treeio: An R Package for Phylogenetic Tree Input and Output with Richly Annotated and Associated Data. Mol Biol Evol. 37(2):599–603.

Warren SD, Clair LL St, Stark LR, Lewis LA, Pombubpa N, Kurbessoian T, Stajich JE, Aanderud ZT. 2019. Reproduction and dispersal of biological soil crust organisms. Front Ecol Evol. 7. doi:10.3389/fevo.2019.00344.

Weber B, Bowker M, Zhang Y, Belnap J. 2016. Natural Recovery of Biological Soil Crusts After Disturbance. In: Weber B, Büdel B, Belnap J, editors. Biological Soil Crusts: An Organizing Principle in Drylands. Cham: Springer International Publishing. p. 479–498.

Wheeler MH. 1983. Comparisons of fungal melanin biosynthesis in ascomycetous, imperfect and basidiomycetous fungi. Trans Br Mycol Soc. 81(1):29–36.

White PM. 2001. California Indians and Their Reservations: An Online Dictionary. San Diego State University Library.

Wick RR, Judd LM, Holt KE. 2019. Performance of neural network basecalling tools for Oxford Nanopore sequencing. Genome Biol. 20(1):129.

Yu G, Smith DK, Zhu H, Guan Y, Lam TT-Y. 2017. Ggtree : An r package for visualization and annotation of phylogenetic trees with their covariates and other associated data. Methods Ecol Evol. 8(1):28–36.

Zhang H, Yohe T, Huang L, Entwistle S, Wu P, Yang Z, Busk PK, Xu Y, Yin Y. 2018. dbCAN2: a meta server for automated carbohydrate-active enzyme annotation. Nucleic Acids Res. 46(W1):W95–W101.

Zhao J, Zeng J, de Hoog GS, Attili-Angelis D, Prenafeta-Boldú FX. 2010. Isolation and identification of black yeasts by enrichment on atmospheres of monoaromatic hydrocarbons. Microb Ecol. 60(1):149–156.

Zimin AV, Marçais G, Puiu D, Roberts M, Salzberg SL, Yorke JA. 2013. The MaSuRCA genome assembler. Bioinformatics. 29(21):2669–2677. doi:10.1093/bioinformatics/btt476. http://dx.doi.org/10.1093/bioinformatics/btt476.

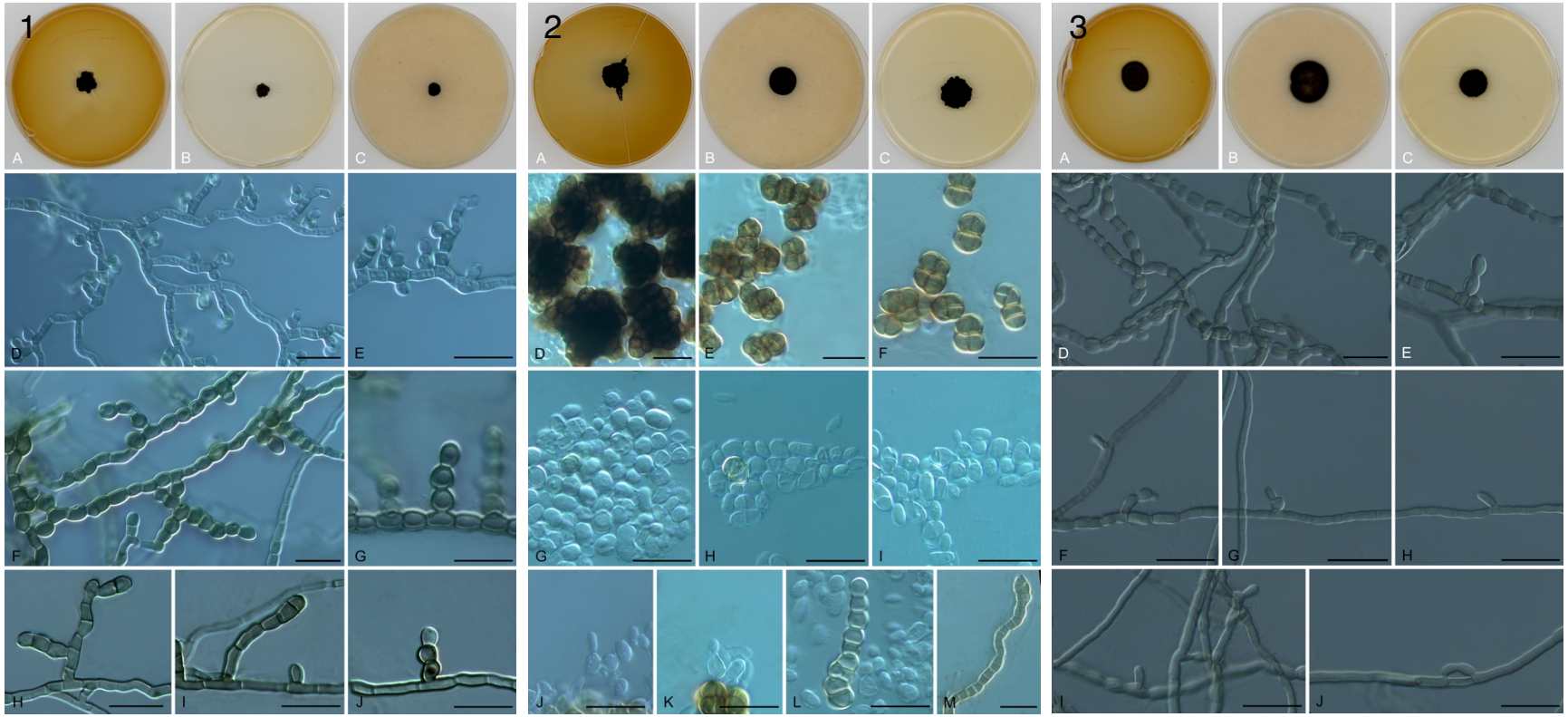
1
A
B
C
D
E
F
G
H
I
J
2
A
B
C
D
E
F
G
H
I
J
K
L
M
3
A
B
C
D
E
F
G
H
I
J

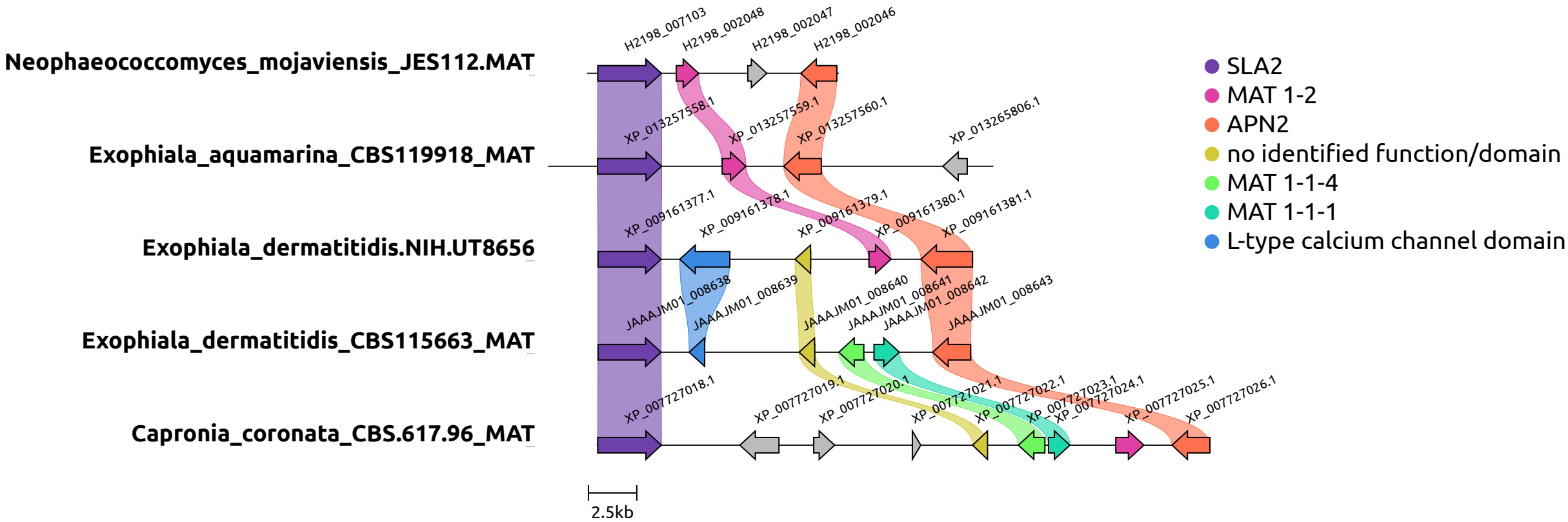
Neophaeococcomyces_mojaviensis_JES112.MAT
Exophiala_aquamarina_CBS119918_MAT
Exophiala_dermatitidis.NIH.UT8656
Exophiala_dermatitidis_CBS115663_MAT
Capronia_coronata_CBS.617.96_MAT
H2198_007103
H2198_002048
H2198_002047
H2198_002046
XP_013257558.1
XP_013257559.1
XP_013257560.1
XP_013265806.1
XP_009161377.1
XP_009161378.1
XP_009161379.1
XP_009161380.1
XP_009161381.1
JAAAJM01_008638
JAAAJM01_008639
JAAAJM01_008640
JAAAJM01_008641
JAAAJM01_008642
JAAAJM01_008643
XP_007727018.1
XP_007727019.1
XP_007727020.1
XP_007727021.1
XP_007727022.1
XP_007727023.1
XP_007727024.1
XP_007727025.1
XP_007727026.1
2.5kb
SLA2
MAT 1-2
APN2
no identified function/domain
MAT 1-1-4
MAT 1-1-1
L-type calcium channel domain

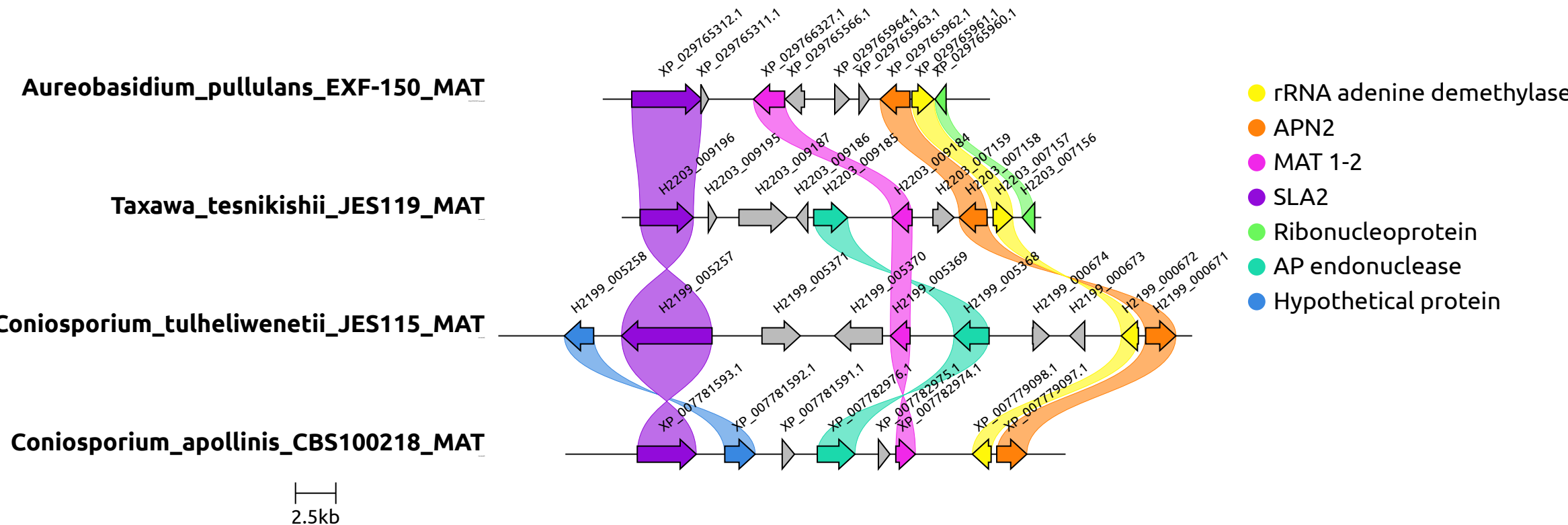
Aureobasidium_pullulans_EXF-150_MAT
Taxawa_tesnikishii_JES119_MAT
Coniosporium_tulheliwenetii_JES115_MAT
Coniosporium_apollinis_CBS100218_MAT
XP_029765312.1
XP_029765311.1
XP_029766327.1
XP_029765566.1
XP_029765964.1
XP_029765963.1
XP_029765962.1
XP_029765961.1
XP_029765960.1
H2203_009196
H2203_009195
H2203_009187
H2203_009186
H2203_009185
H2203_009184
H2203_007159
H2203_007158
H2203_007157
H2203_007156
H2199_005258
H2199_005257
H2199_005371
H2199_005370
H2199_005369
H2199_005368
H2199_000674
H2199_000673
H2199_000672
H2199_000671
XP_007781593.1
XP_007781592.1
XP_007781591.1
XP_007782976.1
XP_007782975.1
XP_007782974.1
XP_007779098.1
XP_007779097.1
2.5kb
rRNA adenine demethylase
APN2
MAT 1-2
SLA2
Ribonucleoprotein
AP endonuclease
Hypothetical protein

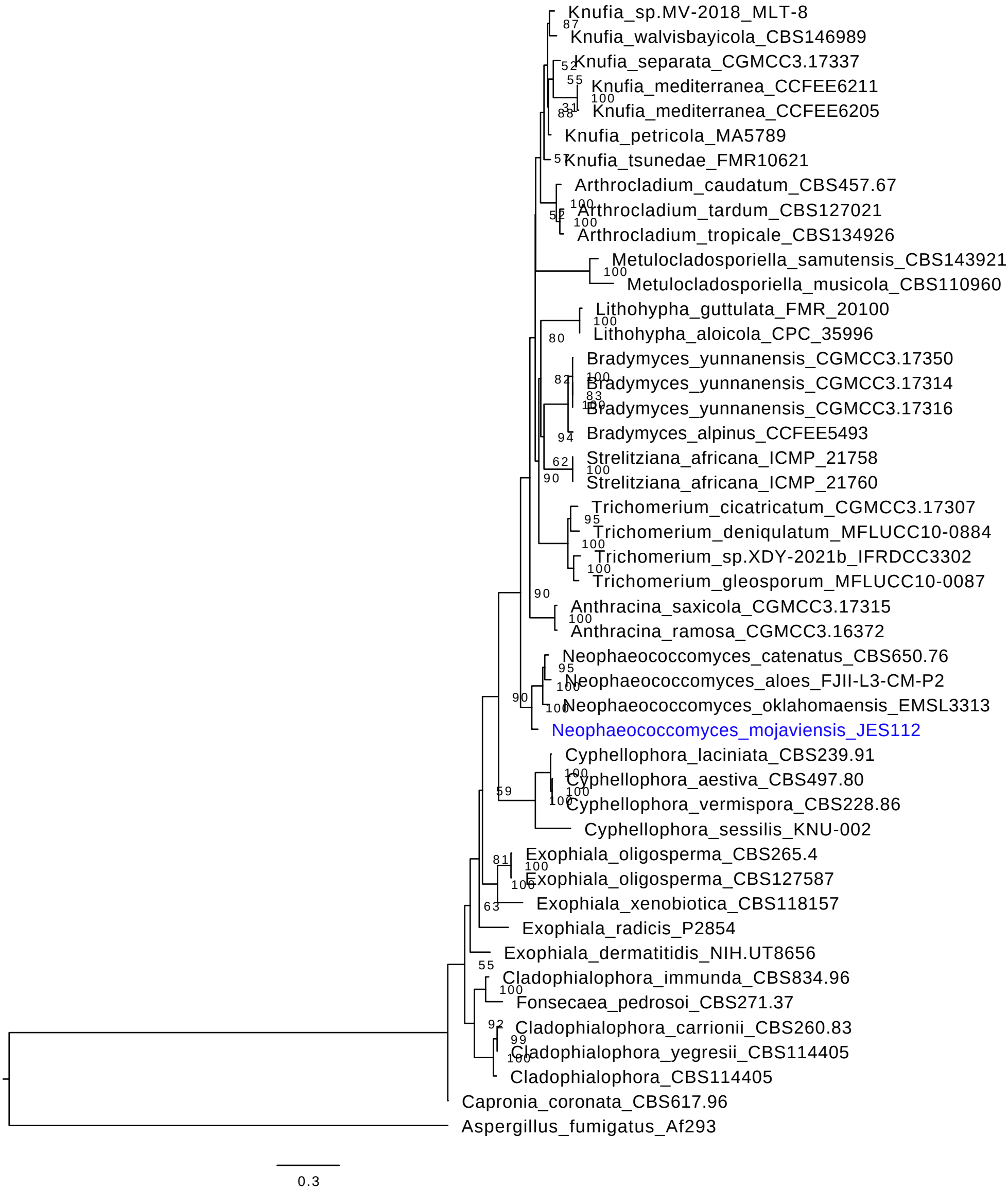
Knufia_sp.MV-2018_MLT-8
87
Knufia_walvisbayicola_CBS146989
Knufia_separata_CGMCC3.17337
52
55
Knufia_mediterranea_CCFEE6211
100
31
88
Knufia_mediterranea_CCFEE6205
Knufia_petricola_MA5789
57
Knufia_tsunedae_FMR10621
Arthrocladium_caudatum_CBS457.67
100
Arthrocladium_tardum_CBS127021
52
100
Arthrocladium_tropicale_CBS134926
Metulocladosporiella_samutensis_CBS143921
100
Metulocladosporiella_musicola_CBS110960
Lithohypha_guttulata_FMR_20100
100
80
Lithohypha_aloicola_CPC_35996
Bradymyces_yunnanensis_CGMCC3.17350
82
100
Bradymyces_yunnanensis_CGMCC3.17314
83
100
Bradymyces_yunnanensis_CGMCC3.17316
94
Bradymyces_alpinus_CCFEE5493
62
Strelitziana_africana_ICMP_21758
100
90
Strelitziana_africana_ICMP_21760
Trichomerium_cicatricatum_CGMCC3.17307
95
Trichomerium_deniqulatum_MFLUCC10-0884
100
Trichomerium_sp.XDY-2021b_IFRDCC3302
100
Trichomerium_gleosporum_MFLUCC10-0087
90
Anthracina_saxicola_CGMCC3.17315
100
Anthracina_ramosa_CGMCC3.16372
Neophaeococcomyces_catenatus_CBS650.76
95
Neophaeococcomyces_aloes_FJII-L3-CM-P2
100
90
100
Neophaeococcomyces_oklahomaensis_EMSL3313
Neophaeococcomyces_mojaviensis_JES112
Cyphellophora_laciniata_CBS239.91
100
Cyphellophora_aestiva_CBS497.80
59
100
100
Cyphellophora_vermispora_CBS228.86
Cyphellophora_sessilis_KNU-002
81
Exophiala_oligosperma_CBS265.4
100
Exophiala_oligosperma_CBS127587
100
63
Exophiala_xenobiotica_CBS118157
Exophiala_radicis_P2854
Exophiala_dermatitidis_NIH.UT8656
55
Cladophialophora_immunda_CBS834.96
100
Fonsecaea_pedrosoi_CBS271.37
92
Cladophialophora_carrionii_CBS260.83
99
Cladophialophora_yegresii_CBS114405
100
Cladophialophora_CBS114405
Capronia_coronata_CBS617.96
Aspergillus_fumigatus_Af293
0.3

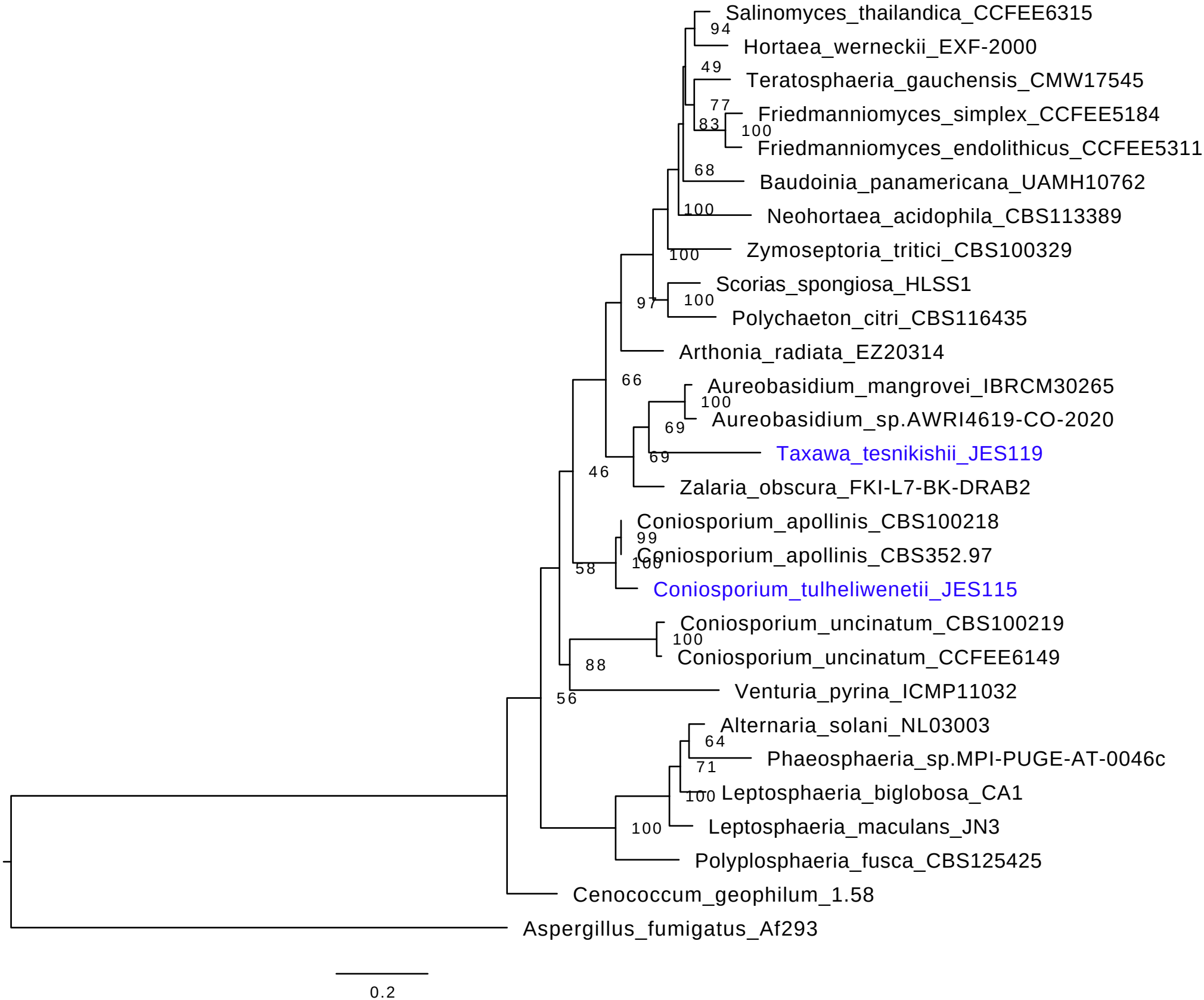
Salinomyces_thailandica_CCFEE6315
94
Hortaea_werneckii_EXF-2000
49
Teratosphaeria_gauchensis_CMW17545
77
Friedmanniomyces_simplex_CCFEE5184
83
100
Friedmanniomyces_endolithicus_CCFEE5311
68
Baudoinia_panamericana_UAMH10762
100
Neohortaea_acidophila_CBS113389
100
Zymoseptoria_tritici_CBS100329
Scorias_spongiosa_HLSS1
97
100
Polychaeton_citri_CBS116435
Arthonia_radiata_EZ20314
66
Aureobasidium_mangrovei_IBRCM30265
100
Aureobasidium_sp.AWRI4619-CO-2020
69
Taxawa_tesnikishii_JES119
69
46
Zalaria_obscura_FKI-L7-BK-DRAB2
Coniosporium_apollinis_CBS100218
99
Coniosporium_apollinis_CBS352.97
100
58
Coniosporium_tulheliwenetii_JES115
Coniosporium_uncinatum_CBS100219
100
Coniosporium_uncinatum_CCFEE6149
88
Venturia_pyrina_ICMP11032
56
Alternaria_solani_NL03003
64
Phaeosphaeria_sp.MPI-PUGE-AT-0046c
71
100
Leptosphaeria_biglobosa_CA1
100
Leptosphaeria_maculans_JN3
Polyplosphaeria_fusca_CBS125425
Cenococcum_geophilum_1.58
Aspergillus_fumigatus_Af293
0.2

Table 1. Three species were collected from biological soil crusts collected from two desert locations in Southern California. Strain JES_112 was isolated from the south east region of Joshua Tree National Park in the Mojave Desert, while JES_115 and JES_119 were both collected from biological soil crusts collected from the campground site in the UC Natural Reserve of Boyd Deep Canyon.

Species	**Date**	**Location**	**Coordinates**
JES_112	November 2017	Joshua Tree National Park, CA	34.1026 °N, -115.4542°W
JES_115	July 2019	Boyd Deep Canyon Reserve, CA	34.0182 °N, -116.0262 °W
JES_119	July 2019	Boyd Deep Canyon Reserve, CA	34.0182 °N, -116.0262 °W

Table 2. Genome assembly and annotation summary statistics. All strains were sequenced with Illumina and Nanopore sequencing. With the added sequencing reads, we were able to glean telomere information along with genome completeness. It is clear that JES_112 is contaminated as the BUSCO score is lower, while JES_115 and JES_119 are much closer to a more complete genome.

	JES_112	**JES_115**	**JES_119**
Scaffold Count	478	64	38
Total Length	32,593,754 bp	32,607,911 bp	29,383,553 bp
Minimum Length	561	4823	1783
Maximum Length	427,480	1,739,523	2,828,030
Mean Scaffold Length	68,187.77	509,498.61	773,251.39
Scaffold L50	87	14	9
Scaffold N50	117,971	966,560	1,232,081
Scaffold L90	282	31	24
Scaffold N90	32,261	507,175	558,687
BUSCO Complete % Illumina	84.7	90.2	97.4
BUSCO Complete % Nanopore	73.4	92.6	92.9
BUSCO Duplicate % Nanopore	0.2	0.1	0.1
BUSCO Single % Nanopore	73.2	92.5	92.8
GC%	48.25	52.55	51.98

Illumina coverage	34.58x	43.45x	25.38x
Nanopore coverage	0.83x	20.44x	194.58x
Telomere Count	0, 0F, 0R	61, 29 F, 32 R	55, 29 F, 26 R
Number of Genes	10,996	9,304	9,386
mRNA genes	10,924	9,226	9,189
tRNA genes	72	78	197
GO Terms	6,001	5,089	5,321
InterProScan	8,523	7,079	7,291
EGGNOG	9,934	8,487	8,511
PFAM	7,520	5,982	6,219
CAZYme	309	257	346
MEROPS	344	284	291
Secretion	674	532	631

Table 3. Predicted secondary metabolite gene clusters. The BGCs predicted include multiple copies of PKS and NRPS genes, but siderophores were only recovered in JES_112. There was a higher number of BGCs predicted in JES_112 (27) our *Chaetothyriales* species, than JES_115 and JES_119 (15) our *Dothideomycetes*. This table lists the numbers of each. JES_112 has a much higher number (27) of secondary metabolites than the other two (15).

	T1PKS	Terpene	T3PKS	NRPS	NRPS-like	Siderophore	Arylpolyene	Betalactone	Fungal RiPP
JES 112	6	6	2	4	6	1	1	1	0
JES 115	5	4	0	2	3	0	0	1	0
JES 119	1	4	0	1	7	0	0	1	1

Table 4. Gene Tree Nucleotide Accession numbers. Collected accession numbers of alternative strains to build Figures 4 and 5. The remaining empty spaces indicate the need to pull the sequences using BLAST. Once collected each gene populated a gene FASTA file, aligned, clipped and IQTREE2, a tree-building program, was run to determine the gene models for each gene. Once determined, the gene alignment lengths were calculated and partitioning scripts were described and used to build a larger tree, using IQTREE2.

Species	**Beta-Tubulin**	**Calmodulin**	**Internal-Transcribed Spacer**	**Large Subunit (Ribosomal)**
*Neophaeococcomyces mojaviensis*JES112	-	-	-	-
Taxawa tesnikishii JES119	-	-	-	-
Alternaria solani NL03003	MK388240.1	MH243808.1	NR_172408.1	ON416546.1
Anthracina ramosa CGMCC3.16372	KP226556.1	-	NR_172152.1	KP174923.1
Anthracina saxicola CGMCC3.17315	KP226554.1	-	NR_172151.1	KP174921.1
Arthrocladium caudatum CBS457.67	LT558710.1	-	NR_145398.1	MH870732.1
Arthrocladium tardum CBS 127021	-	-	NR_154706.1	NG_057089.1
Arthrocladium tropicale CBS 134926	KX822406.1	-	NR_154724.1	NG_057119.1
Aureobasidium mangrovei IBRCM30265	XM_029904852.1	XM_041025809.1	NR_174637.1	NG_078639.1
*Aureobasidium sp.*AWRI4619-CO-2020	XM_029904852.1	XM_041025809.1	MK256457.1	MK968773.1
Baudoinia panamericana UAMH10762	XM_007673885.1	XM_007675264.1	NR_153615.1	KT186497.1
Bradymyces alpinus CCFEE 5493	LN589970.1	-	NR_132844.1	NG_058641.1

Bradymyces yunnanensis CGMCC 3.17350	KP226545.1	-	KP174865.1	KP174926.1
Capronia coronata CBS 617.96	XM_007728982.1	XM_007721556.1	NR_154745.1	NG_067831.1
Cenococcum geophilum 1.58	-	-	KC967410.1	MN817694.1
Cladophialophora carrionii CBS 260.83	KF928582.1	XM_008724000.1	MH861582.1	MH873312.1
Cladophialophora_yegresii CBS 114405	EU137209.1	-	NR_111284.1	KX822323.1
Cladophialophora immunda CBS 834.96	EU137203.1	-	NR_111283.1	MH874242.1
Coniosporium apollinis CBS 100218	-	XM_007785495.1	NR_159787.1	GU250898.1
Coniosporium uncinatum CBS 100219	-	-	NR_145343.1	NG_058806.1
Coniosporium uncinatum CCFEE 6149	-	-	MZ573424.1	MZ573424.1
Cyphellophora aestiva CBS 239.91	MW297547.1	-	MH861291.1	MH873056.1
Cyphellophora laciniata CBS 239.91	KF928604.1	-	NR_121335.1	MH873933.1
Cyphellophora sessilis KNU-002	KX431943.1	-	KX431941.1	KX431942.1
Cyphellophora vermispora CBS 228.86	KC455227.1	-	KC455244.1	KC455257.1
Exophiala dermatitidis NIH.UT8656	-	XM_009160450.1	JH226131.1	ON543213.1
Exophiala oligosperma CBS 265.49	EF551507.1	XM_016404560.1	MH856519.1	MH868049.1

Exophiala oligosperma CBS 127587	KF928570.1	-	MH864631.1	MH876068.1
Exophiala radicis P2854	KT723463.1	-	NR_158397.1	NG_069319.1
Exophiala xenobiotica CBS 118157	NW_013562490.1	XM_013454656.1	OP132917.1	MH875251.1
Fonsecaea pedrosoi CBS 271.37	XM_013430809.1	XM_013426864.1	MT023597.1	KF155185.1
Friedmanniomyces endolithicus CCFEE 5311	-	-	NR_144917.1	GU250367.1
Friedmanniomyces simplex CCFEE 5184	-	-	NR_155079.1	GU250368.1
Hortaea werneckii EXF-2000	-	-	NR_145338.1	NG_057773.1
Knufia petricola MA5789	-	-	NR_111871.1	MT126669.1
Knufia mediterranea CCFEE 6211	-	-	KP791793.1	KR781080.1
Knufia mediterranea CCFEE 6205	-	-	KP791794.1	KR781081.1
Knufia separata CGMCC 3.17337	KP226564.1	-	NR_172233.1	KP174931.1
Knufia tsunedae FMR10621	-	-	NR_132842.1	HG003672.1
Knufia walvisbayicola CBS 146989	MZ078266.1	-	NR_173046.1	NG_076737.1
Knufia sp. MV-2018 MLT-8	-	-	MT636977.1	MT636937.1
Leptosphaeria biglobosa CA1	AY749005.1	-	NR_111620.1	JX681093.1
Leptosphaeria maculans JN3	AY749012.1	XM_003840719.1	M96384.1	JF740306.1

Lithohypha aloicola CPC35996	MN556837.1	-	NR_166313.1	NG_068316.1
Lithohypha guttulata FMR 20100	OX346320.1	-	OX346376.1	OX346377.1
Metulocladosporiella musicola CBS 110960	-	MG934537.1	MH862870.1	NG_067447.1
Metulocladosporiella samutensis CBS 143921	-	MG934540.1	NR_161056.1	MG934453.1
Neohortaea acidophila CBS 113389	XM_033733287.1	XM_033733930.1	NR_169648.1	OL739260.1
Neophaeococcomyces aloes FJII-L3-CM-P2	-	-	NR_132069.1	KF777234.1
Neophaeococcomyces catenatus CBS 650.76	-	-	AF050277.1	MH872793.1
Neophaeococcomyces oklahomaensis EMSL3313	-	-	MW798187.1	MW798182.1
*Phaeosphaeria sp.*MPI-PUGE-AT-0046c	-	-	NR_155675.1	NG_068582.1
Polychaeton citri CBS 116435	-	-	GU214649.1	OM238161.1
Polyplosphaeria fusca CBS 125425	-	-	NR_119397.1	MH875147.1
Salinomyces thailandica CCFEE 6315	-	-	NR_171710.1	MH875167.1
Scorias spongiosa HLSS1	-	-	NR_154422.1	MH866910.1
Strelitziana africana ICMP 21758	-	-	MK210538.1	MK210499.1
Strelitziana africana ICMP 21760	-	-	MK210540.1	MK210501.1

Teratosphaeria gauchensis CMW 17545	-	KF902726.1	NR_144976.1	EU019295.2
Trichomerium cicatricatum CGMCC3.17307	KP226540.1	-	NR_172232.1	KP174947.1
Trichomerium deniqulatum MFLUCC10-0884	-	-	NR_132965.1	NG_059479.1
Trichomerium gleosproum MFLUCC10-0087	-	-	JX313656.1	JX313662.1
Trichomerium sp. XDY-2021a-IFRDCC3302	-	-	MN901488.1	MZ822131.1
Tuber melanosporum	MZ458420.1	XM_002841184.1	GQ917052.1	JF807486.1
Venturia pyrina ICMP11032	EU853839.1	-	NR_169905.1	AY849967.1
Zalaria obscura FKI-L7-BK-DRAB2	-	-	NR_153466.1	MT103097.1
Zymoseptoria tritici CBS 100329	XM_003856727.1	KF254299.1	KP852517.1	MK788267.1